2011 50th IEEE Conference on Decision and Control and
European Control Conference (CDC-ECC)
Orlando, FL, USA, December 12-15, 2011

Lead-Lag compensators: analytical and graphical design on the Nyquist plane

Roberto Zanasi, Stefania Cuoghi and Lorenzo Ntogramatzidis

Abstract— **This paper presents a design method for the synthesis of a general class of lead-lag compensators to exactly satisfy gain and phase margins specifications. A free parameter of the compensator is used as a degree of freedom in order to satisfy additional requirements on the phase and/or gain crossover frequencies. A graphical procedure for the compensator design on the Nyquist plane is presented with some numerical examples.**

I. INTRODUCTION

From classical control theory, it is known that the gain and phase margins (GPM) serve as important measures of the robustness of a dynamical system. The phase margin is related to the damping of the system, and therefore also serves as performance measurement [1]. Different methods can be found in the literature to satisfy GPM specifications [2]-[5]. However such solutions are usually obtained with trial-and-error methods. In 1998 a graphical method for the design of lead-lag compensators to satisfy GPM specifications was presented [2]. The recent literature shows a renewed interest in the design of classical controllers [6]-[9]. In these papers both a numerical and a graphical solution to the design of lead-lag compensators based on GPM specifications is proposed. A general structure for the lead-lag compensator with real and complex zeros and poles is used, relating it to the classical form with real zeros and poles. The paper is organized as follows: in Section II, the basic properties of this general form of lead-lag compensator are presented. In Section III the inversion formulae and their properties are described. In Section IV the design problems with constraints on the GPM are introduced, and their solutions are presented along with a graphical representation. Numerical examples and conclusions end the paper.

This work was partially supported by the Australian Research Council (Discovery Grant DP0986577).

R. Zanasi and S. Cuoghi are with the Faculty of Engineering, DII-Information Engineering Department, University of Modena and Reggio Emilia Via Vignolese 905, 41100, Modena, Italy, e-mails: roberto.zanasi@unimore.it and stefania.cuoghi@unimore.it.

L. Ntogramatzidis is with the Department of Mathematics and Statistics, Curtin University, Perth, WA, Australia, e-mail: L.Ntogramatzidis@curtin.edu.au.

II. LEAD-LAG COMPENSATORS: THE GENERAL STRUCTURE

Consider a lead-lag compensator described by the transfer function

$$C(s) = \frac{s^2 + 2\gamma\delta\omega_n s + \omega_n^2}{s^2 + 2\delta\omega_n s + \omega_n^2}, \qquad (1)$$

where γ, δ and ω_n are real and positive. The coefficients $\gamma\delta$ and δ are the damping ratios of the numerator and the denominator. When $\gamma\delta < 1$ and/or $\delta < 1$ the zeros and/or the poles of the lead-lag compensator $C(s)$ are complex conjugate with negative real part. The compensator $C(s)$ has a unity static gain $C(0) = 1$ which does not change the static behavior of the controlled system. Notice that the compensator C(s) is written in a general form which encompasses the classical lead-lag form $C_r(s)$ with real poles and real zeros:

$$C_r(s) = \frac{(1+\tau_1 s)(1+\tau_2 s)}{(1+\alpha\tau_1 s)(1+\frac{\tau_2}{\alpha}s)} \qquad (2)$$

where $0 < \tau_1 < \tau_2$ and $0 < \alpha < 1$. The relations that link the parameters in (1) and (2) are:

$$\tau_1 = \frac{\gamma\delta - \sqrt{\gamma^2\delta^2 - 1}}{\omega_n}, \qquad \tau_2 = \frac{\gamma\delta + \sqrt{\gamma^2\delta^2 - 1}}{\omega_n},$$

$$\alpha = \frac{\delta - \sqrt{\delta^2 - 1}}{\gamma\delta - \sqrt{\gamma^2\delta^2 - 1}}.$$

The frequency response of compensator $C(s)$ is

$$C(j\omega) = \frac{1 + jX(\omega)}{1 + jY(\omega)}, \qquad (3)$$

where

$$X(\omega) = \frac{2\gamma\delta\,\omega\,\omega_n}{\omega_n^2 - \omega^2}, \qquad Y(\omega) = \frac{2\delta\,\omega\,\omega_n}{\omega_n^2 - \omega^2}. \qquad (4)$$

Since γ, δ and ω_n are assumed to be real and positive, $X(\omega)$ and $Y(\omega)$ are positive when $\omega < \omega_n$ and negative when $\omega > \omega_n$. The Nyquist diagram of $C(j\omega)$ is a circle $C(\gamma)$ with center $C_0 = \frac{\gamma+1}{2}$ and radius $R_0 = \frac{|\gamma-1|}{2}$ (see Fig 1), that is

$$C(\gamma) = C_0 + R_0 e^{j\theta} \qquad \forall\theta \in [0, 2\pi]. \qquad (5)$$

Proof: The distance d of the generic point $C(j\omega)$ from the point C_0 is constant and equal to R_0:

$$d^2 = |C(j\omega) - C_0|^2 = \left| \frac{\omega_n^2 - \omega^2 + j\,2\gamma\delta\omega_n\omega}{\omega_n^2 - \omega^2 + j\,2\delta\omega_n\omega} - \frac{\gamma+1}{2} \right|^2$$

$$= \left| \frac{(1-\gamma)[(\omega_n^2 - \omega^2) - j\,2\gamma\delta\omega_n\omega)]}{2(\omega_n^2 - \omega^2 + j\,2\delta\omega_n\omega)} \right|^2 = \left| \frac{\gamma-1}{2} \right|^2 = R_0^2.$$

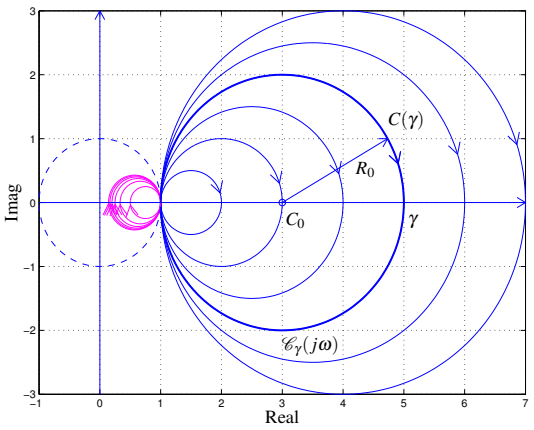

Fig. 1. Nyquist diagrams of $C(j\omega)$ when $\omega_n = 1$, ($\delta = 1.5$, $\gamma = [2:1:7]$, blue lines) and ($\delta = 1.5$, $\gamma = 1./[2:1:7]$, magenta lines). The thick blue line corresponds to $\delta = 1.5$ and $\gamma = 5$.

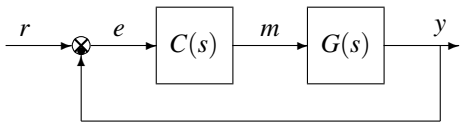

Fig. 2. Unity feedback control structure.

The shape of $C(\gamma)$ does not depend on $\delta > 0$ and $\omega_n > 0$. The intersections of $C(j\omega)$ with the real axis occur at points 1 and γ. Notice that the value of γ denotes the minimum (or maximum) amplitude of $C(j\omega)$ when $\gamma < 1$ (or $\gamma > 1$) and is the gain of the compensator $C(s)$ for $\omega = \omega_n$:

$$\gamma = C(j\omega_n) = \lim_{\omega \to \omega_n} \frac{X(\omega)}{Y(\omega)}. \tag{6}$$

Let $\mathscr{C}(\gamma)$ denote the set of all the compensators $C(s)$ having the same parameter γ, that is

$$\mathscr{C}(\gamma) = \left\{ C(s) \text{ as in } (1) \;\middle|\; \delta > 0, \omega_n > 0 \right\}. \tag{7}$$

Moreover, let $\mathscr{C}_\gamma(s) \in \mathscr{C}(\gamma)$ denote one element of set $\mathscr{C}(\gamma)$ chosen arbitrarily. In Fig. 1 the circle $\mathscr{C}_\gamma(j\omega)$ represents the frequency response of the generic functions $\mathscr{C}_\gamma(s) \in \mathscr{C}(\gamma)$.

III. Lead-lag compensators $C(s, \omega_n)$ moving a point A to a point B

Consider the block-diagram shown in Fig. 2, where $G(s)$ denotes the transfer function of the LTI plant to be controlled, which may include the gain and the integration terms required to meet the steady-state accuracy specifications. The lead-lag compensator $C(s)$ has to be designed in order to satisfy phase margin ϕ_m, the gain margin G_m and the gain or phase crossover frequency specifications. For this purpose a gain term or a first order regulator are not enough. Let $C(j\omega_0) = M_0 e^{j\varphi_0}$ denote the value of the frequency response

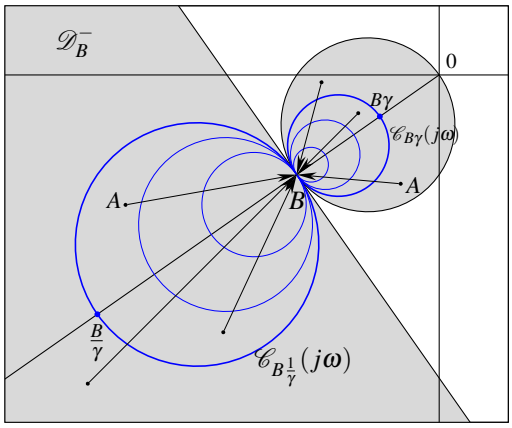

Fig. 3. Controllable domain $\mathscr{D}_B^- = \mathscr{D}_{B1}^- \cup \mathscr{D}_{B2}^-$ of lead-lag compensator $C(s)$ on the Nyquist plane.

$C(j\omega) = M(\omega) e^{j\varphi(\omega)}$ at frequency ω_0, where $M_0 = M(\omega_0)$ and $\varphi_0 = \varphi(\omega_0)$. To study how $C(j\omega_0)$ affects $G(j\omega)$ at frequency ω_0, let us consider two generic points $A = M_A e^{j\varphi_A}$ and $B = M_B e^{j\varphi_B}$ of the complex plane. Referring to Fig. 3, we say that *point A is controllable to point B* (or equivalently that *point A can be moved to point B*) if a value $C(j\omega_0)$ exists such that

$$B = C(j\omega_0) \cdot A, \tag{8}$$

that is if and only if the following conditions hold:

$$M_B = M_A M_0, \qquad \varphi_B = \varphi_A + \varphi_0. \tag{9}$$

Definition 1: ($\mathscr{D}_B^-$) Given a point $B \in \mathbb{C}$, let us define "*controllable domain of lead-lag compensator $C(s)$ to point B*" as

$$\mathscr{D}_B^- = \left\{ A \in \mathbb{C} \;\middle|\; \exists\, \gamma, \delta, \omega_n > 0, \exists\, \omega \geq 0 : C(j\omega) \cdot A = B \right\}$$

△

It is easy to see that domain $\mathscr{D}_B^-$ can be expressed, see the gray regions in Fig. 3, as $\mathscr{D}_B^- = \mathscr{D}_{B1}^- \cup \mathscr{D}_{B2}^-$ where

$$\mathscr{D}_{B1}^- = \left\{ A = M_A e^{j\varphi_A} \;\middle|\; -\frac{\pi}{2} + \varphi_B < \varphi_A < \frac{\pi}{2} + \varphi_B, \; M_A > \frac{M_B}{\cos(\varphi_A - \varphi_B)} \right\},$$

$$\mathscr{D}_{B2}^- = \left\{ A = M_A e^{j\varphi_A} \;\middle|\; -\frac{\pi}{2} + \varphi_B < \varphi_A < \frac{\pi}{2} + \varphi_B, \; 0 < M_A < M_B \cos(\varphi_A - \varphi_B) \right\}.$$

Definition 2: Given a point $B \in \mathbb{C}$, let $\mathscr{C}_B(\gamma)$ and $\mathscr{C}_B^-(\gamma)$ denote the sets of lead-lag compensators $C_B(s)$ and $C_{B^{-1}}(s)$ defined as follows

$$\mathscr{C}_B(\gamma) = \left\{ C_B(s) = B \cdot C(s) \;\middle|\; C(s) \in \mathscr{C}(\gamma) \right\} \tag{10}$$

$$\mathscr{C}_B^-(\gamma) = \left\{ C_{B^{-1}}(s) = \frac{B}{C(s)} \;\middle|\; C(s) \in \mathscr{C}(\gamma) \right\} \tag{11}$$

with $\mathscr{C}(\gamma)$ defined in (7). Moreover, let $\mathscr{C}_{B\gamma}(s) \in \mathscr{C}_B(\gamma)$ and $\mathscr{C}^-_{B\gamma}(s) \in \mathscr{C}^-_B(\gamma)$ denote particular elements of the two sets $\mathscr{C}_B(\gamma)$ and $\mathscr{C}^-_B(\gamma)$ chosen arbitrarily.

Property 1: *Given $\gamma > 0$, the two sets $\mathscr{C}^-_B(\gamma)$ and $\mathscr{C}_B(\frac{1}{\gamma})$ coincide, i.e.,*

$$\mathscr{C}^-_B(\gamma) = \mathscr{C}_B(\tfrac{1}{\gamma}) \tag{12}$$

and therefore the Nyquist diagrams of functions $\mathscr{C}^-_{B\gamma}(j\omega)$ and $\mathscr{C}_{B\frac{1}{\gamma}}(j\omega)$ corresponding to $\mathscr{C}^-_{B\gamma}(s)$ and $\mathscr{C}_{B\frac{1}{\gamma}}(s)$, respectively, have the same shape. The intersections p_1 and p_2 of $\mathscr{C}^-_{B\gamma}(j\omega)$ with the straight line r passing through points 0 and B are $p_1 = B$ and $p_2 = \frac{B}{\gamma}$, respectively. The corresponding graphical representation is shown in Fig. 3.

Proof: Each element $\mathscr{C}^-_{B\gamma}(s)$ of the set $\mathscr{C}^-_B(\gamma)$ also belongs to the set $\mathscr{C}_B(\frac{1}{\gamma})$. In fact, from (7), (10) and (11), it follows that

$$\begin{aligned}\mathscr{C}^-_{B\gamma}(s) &= B\,\frac{s^2+2\delta\omega_n s+\omega_n^2}{s^2+2\gamma\delta\omega_n s+\omega_n^2}\bigg|_{\substack{\forall\delta>0\\ \forall\omega_n>0}} \\ &= B\,\frac{s^2+2(\frac{1}{\gamma})\bar{\delta}\omega_n s+\omega_n^2}{s^2+2\bar{\delta}\omega_n s+\omega_n^2}\bigg|_{\substack{\forall\bar{\delta}>0\\ \forall\omega_n>0}} \in \mathscr{C}_B(\tfrac{1}{\gamma}),\end{aligned}$$

where $\bar{\delta} = \gamma\delta$. In the same way it can be easily proved that each element $\mathscr{C}_{B\frac{1}{\gamma}}(s)$ of $\mathscr{C}_B(\frac{1}{\gamma})$ also belongs to $\mathscr{C}^-_B(\gamma)$, and therefore $\mathscr{C}^-_B(\gamma)$ and $\mathscr{C}_B(\frac{1}{\gamma})$ coincide. Moreover, the shape of the Nyquist diagrams of $\mathscr{C}^-_{B\gamma}(s)$ and $\mathscr{C}_{B\frac{1}{\gamma}}(s)$ depend only on γ and therefore they coincide. From (5) and (12) it follows that the Nyquist diagram of $\mathscr{C}^-_{B\gamma}(s)$ is a circle whose center $C_0 = B(\gamma+1)/(2\gamma)$ lies on the axis r passing through points O and B, whose radius is $R_0 = |\gamma-1|/(2\gamma)$ and its intersections with the axis r occur at points $a = B$ and $b = \frac{B}{\gamma}$, see Fig. 3. □

Definition 3: ***(Inversion Formulae)*** Given two points $A = M_A e^{j\varphi_A}$ and $B = M_B e^{j\varphi_B}$ of the complex plane $\mathbb{C}$, the inversion formulae $X(A,B)$ and $Y(A,B)$ are defined as

$$\begin{aligned} X(A,B) &= \frac{M-\cos\varphi}{\sin\varphi}, \\ Y(A,B) &= \frac{\cos\varphi-\frac{1}{M}}{\sin\varphi}, \end{aligned} \tag{13}$$

where $M = \frac{M_B}{M_A}$ and $\varphi = \varphi_B - \varphi_A$.

△

These equations are the same inversion formulae for the continuous-time case introduced in [10] and used in [11] and [12].

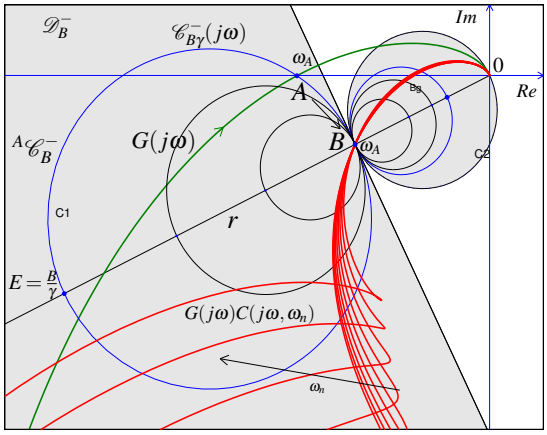

Fig. 4. Design of the lead-lag compensators $C(j\omega,\omega_n)$ moving point A to point B.

Property 2: ***(From A to B)*** *Given a point $B \in \mathbb{C}$ and chosen a point A of the frequency response $G(j\omega)$ at frequency ω_A belonging to the controllable domain $\mathscr{D}^-_B$, i.e., $A = G(j\omega_A) \in \mathscr{D}^-_B$, the set $C(s,\omega_n)$ of all the lead-lag compensators $C(s)$ that move point A to point B is obtained from (1) using the parameters*

$$\gamma = \frac{X}{Y} > 0, \qquad \delta = Y\,\frac{\omega_n^2-\omega_A^2}{2\omega_n\omega_A} > 0 \tag{14}$$

for all $\omega_n > 0$ such that $\delta > 0$ and with parameters $X = X(A,B)$ and $Y = Y(A,B)$ obtained using the inversion formulae (13).

Proof: For $\omega = \omega_A$, (4) can be rewritten as

$$\gamma = \frac{X(\omega_A)}{Y(\omega_A)}, \qquad \delta = Y(\omega_A)\,\frac{\omega_n^2-\omega_A^2}{2\omega_n\omega_A}.$$

Substituting in (1) yields

$$C(s,\omega_n) = \frac{s^2 + X(\omega_A)\frac{\omega_n^2-\omega_A^2}{\omega_A}s + \omega_n^2}{s^2 + Y(\omega_A)\frac{\omega_n^2-\omega_A^2}{\omega_A}s + \omega_n^2}.$$

The frequency response of $C(s,\omega_n)$ at frequency ω_A is equal to the constant value

$$C(j\omega_A,\omega_n) = C(j\omega_A) = \frac{1+jX}{1+jY}. \tag{15}$$

From (8) and (9) it is evident that point $A = G(j\omega_A) = M_A e^{j\varphi_A}$ can be moved to point $B = M_B e^{j\varphi_B}$ if and only if

$$C(j\omega_A) = M e^{j\varphi} = \frac{M_B}{M_A} e^{j(\varphi_B-\varphi_A)}. \tag{16}$$

From (15) and (16) we obtain the inversion formulae $X = X(A,B)$ and $Y = Y(A,B)$ introduced in Definition 3. The hypothesis that point A belongs to the controllable domain $\mathscr{D}^-_B$ ensures, see Definition 1, that there exist admissible lead-lag controllers $C(s,\omega_n)$ moving point A to point B which are characterized by positive parameters γ,

δ and ω_n. All the admissible values of ω_n are those which in (14) satisfy $\delta > 0$. □

IV. Design Problem (ϕ_m , G_m) and Graphical Representations.

Design Problem (ϕ_m , G_m): Given the control scheme of Fig. 2, the transfer function $G(s)$ and the design specifications on the phase margin ϕ_m and gain margin G_m, design a lead-lag compensator $C(s)$ such that the loop gain transfer function $C(j\omega)G(j\omega)$ passes through points $B_p = e^{j(\pi+\phi_m)}$ and $B_g = -1/G_m$.

Solution: *let $B_p = e^{j(\pi+\phi_m)}$ and $B_g = -1/G_m = M_{B_g} e^{j\varphi_{B_g}}$ denote the points corresponding to the desired phase margin ϕ_m and gain margin G_m. The set $C_\gamma(s,\omega_p,\omega_g)$ of all the compensators $C(s)$ which solve this Design Problem is obtained as follows.*

a) *Find all the pairs $(\omega_p,\ \omega_g) \in S_{\gamma\omega}$ of frequencies which solve the equation*

$$\gamma = \gamma_p(\omega_p) = \gamma_g(\omega_g), \tag{17}$$

where the gain $\gamma > 0$ is chosen arbitrarily, $S_{\gamma\omega}$ is the set of all the pairs $(\omega_p,\ \omega_g)$ satisfying (17), and functions $\gamma_p(\omega_p)$ and $\gamma_g(\omega_g)$ are defined as

$$\gamma_p(\omega_p) = \frac{X_p}{Y_p}, \qquad \gamma_g(\omega_g) = \frac{X_g}{Y_g}, \tag{18}$$

where the coefficients $X_p = X(A_p(\omega_p),B_p)$, $Y_p = Y(A_p(\omega_p),B_p)$, $X_g = X(A_g(\omega_g),B_g)$ and $Y_g = Y(A_g(\omega_g),B_g)$ are obtained using the inversion formulae (13), $A_p = G(j\omega_p) = M_{A_p}(\omega_p)\, e^{j\varphi_{A_p}(\omega_p)}$ and $A_g = G(j\omega_g) = M_{A_g}(\omega_g)\, e^{j\varphi_{A_g}(\omega_g)}$.

b) *For each pair $(\omega_p,\ \omega_g) \in S_{\gamma\omega}$ compute*

$$\omega_n = \sqrt{\frac{X_g\,\omega_g - X_p\,\omega_p}{\frac{X_g}{\omega_g} - \frac{X_p}{\omega_p}}} = \sqrt{\frac{Y_g\,\omega_g - Y_p\,\omega_p}{\frac{Y_g}{\omega_g} - \frac{Y_p}{\omega_p}}} > 0, \tag{19}$$

$$\delta = Y_p \frac{\omega_n^2 - \omega_p^2}{2\omega_n\omega_p} = Y_g \frac{\omega_n^2 - \omega_g^2}{2\omega_n\omega_g} > 0. \tag{20}$$

A solution $C_\gamma(s,\omega_p,\omega_g)$ of Design Problem (ϕ_m , G_m) exists only if: ***1)*** *γ satisfies*

$$0 < \gamma < \min\left[\max(\gamma_p(\omega_p)), \max(\gamma_g(\omega_g))\right] \tag{21}$$

2) *$S_{\gamma\omega}$ is not empty.* ***3)*** *Points $A_p(\omega_p)$ and $A_g(\omega_g)$ belong, respectively, to the controllable domains $\mathscr{D}_{B_p}^-$ and $\mathscr{D}_{B_g}^-$.* ***4)*** *Parameters ω_n in (19) and δ in (20) are real and positive.*

Proof: The design specifications on the phase margin ϕ_m and gain margin G_m completely define the position of points B_p and B_g on the complex plane. A solution $C_\gamma(s,\omega_p,\omega_g)$ exists only if the frequencies ω_p and ω_g satisfy

$$G(j\omega_p)C_\gamma(j\omega_p) = B_p, \quad G(j\omega_g)C_\gamma(j\omega_g) = B_g, \tag{22}$$

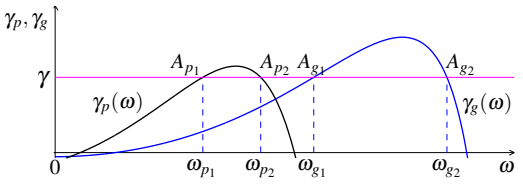

Fig. 5. Functions $\gamma_g(\omega)$ (blue line) and $\gamma_p(\omega)$ (black line).

that is only if $C(s)$ moves point $A_p = G(j\omega_p)$ to point B_p and point $A_g = G(j\omega_g)$ to point B_g. The first condition is verified when γ and δ are obtained from Property 2 when $\omega_A = \omega_p$, $A = A_p$ and $B = B_p$, the second when $\omega_A = \omega_g$, $A = A_g$ and $B = B_g$:

$$\gamma = \gamma_p(\omega_p) = \frac{X_p}{Y_p}, \qquad \delta = Y_p \frac{\omega_n^2 - \omega_p^2}{\omega_p}, \tag{23}$$

$$\gamma = \gamma_g(\omega_g) = \frac{X_g}{Y_g}, \qquad \delta = Y_g \frac{\omega_n^2 - \omega_g^2}{\omega_g}, \tag{24}$$

where the coefficients $X_p = X(A_p(\omega_p),B_p)$, $Y_p = Y(A_p(\omega_p),B_p)$, $X_g = X(A_g(\omega_g),B_g)$ and $Y_g = Y(A_g(\omega_g),B_g)$ are obtained using the inversion formulae (13). Relations (23) and (24) lead directly to (17) and (20). Solving (20) with respect to ω_n leads to the expression of ω_n given in (19). For each value of γ satisfying (21), one can find the set $S_{\gamma\omega}$ of all the solutions (ω_p,ω_g) of (17). This relation does not depend on δ and ω_n, but only on the pairs (ω_p,ω_g) and points $(B_p,\ B_g)$. Each solution $(\omega_p,\omega_g) \in S_{\gamma\omega}$ corresponds to an acceptable regulator $C_\gamma(s,\omega_p,\omega_g)$ only if points A_p and A_g belong respectively to the controllable domains $\mathscr{D}_{B_p}^-$ and $\mathscr{D}_{B_g}^-$, according to Definition 1, and ω_n and δ given in (19) and (20) are real and positive, as assumed in (1). □

The numerical solution of (17) can be obtained graphically by plotting $\gamma_p(\omega)$ and $\gamma_g(\omega)$ and by finding, for each admissible value of γ, all the pairs $(\omega_p,\omega_g) \in S_{\omega_p}$ where $\gamma_p(\omega_p)$ and $\gamma_g(\omega_g)$ intersect the horizontal line γ, see Fig. 5. In the example of Fig. 5 there are four different solutions: $S_{\gamma\omega} = \{(\omega_{p1},\omega_{g1}),(\omega_{p1},\omega_{g2}),(\omega_{p2},\omega_{g1}),(\omega_{p2},\omega_{g2})\}$. The loop gain frequency responses $H_{11}(s)$, $H_{12}(s)$, $H_{21}(s)$ and $H_{22}(s)$ of these four solutions on the Nyquist plane are shown in Fig. 6. These solutions are acceptable only if constraints $\delta > 0$ and $\omega_n > 0$ given in (19) and (20) are satisfied.

A. Graphical Solution on the Nyquist plane.

The graphical solution of (17) can also be obtained using the graphical construction shown in Fig. 6:

1) Given points B_p and B_g and chosen a desired value $\gamma > 0$, draw the circles having their diameters on the segments $(B_p,\ B_p/\gamma)$ and $(B_g,\ B_g/\gamma)$. From Property 1 they coincide with the frequency

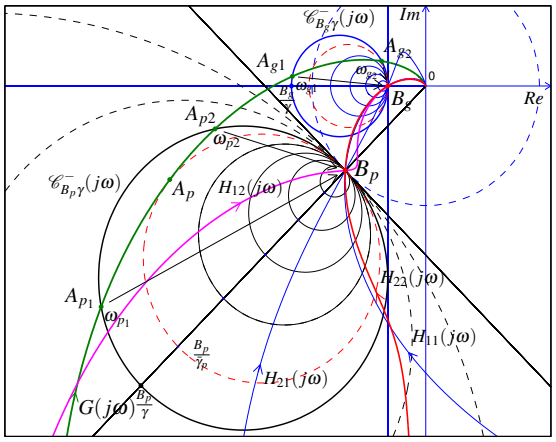

Fig. 6. Graphical determination of frequencies (ω_p, ω_g) on the Nyquist plane. Loop gain frequency response $H_{11}(s)$, $H_{12}(s)$, $H_{21}(s)$ and $H_{22}(s)$ satisfy desired phase and gain margin.

responses of functions $\mathscr{C}^-_{B_p\gamma}(j\omega)$ and $\mathscr{C}^-_{B_g\gamma}(j\omega)$.

2) If the frequency response $G(j\omega)$ does not intersect both circles $\mathscr{C}^-_{B_p\gamma}(j\omega)$ and $\mathscr{C}^-_{B_g\gamma}(j\omega)$, the chosen value of γ is not acceptable.

3) Otherwise, each pair (ω_p, ω_g) corresponding to the intersections of $G(j\omega)$ with circles $\mathscr{C}^-_{B_p\gamma}(j\omega)$ and $\mathscr{C}^-_{B_g\gamma}(j\omega)$ is a possible solution for the Design Problem $(\phi_m\ ,\ G_m)$.

This graphical construction hinges on the fact that frequencies ω_p and ω_g satisfy (22), which can be rewritten as

$$\begin{cases} G(j\omega)|_{\omega=\omega_p} = \dfrac{B_p}{C_\gamma(j\omega_p)} = \mathscr{C}^-_{B_p\gamma}(j\omega)\Big|_{\omega=\omega_p} \\ G(j\omega)|_{\omega=\omega_g} = \dfrac{B_g}{C_\gamma(j\omega_g)} = \mathscr{C}^-_{B_g\gamma}(j\omega)\Big|_{\omega=\omega_g} \end{cases} \tag{25}$$

The Solution of the Design Problem $(\phi_m\ ,\ G_m)$ is also useful for solving, for example, the following Design Problems:

A) Design a lead-lag compensator $C(s)$ which satisfies constraints on the phase margin ϕ_m, the gain margin G_m and the gain crossover frequency ω_p. **Solution**: $\gamma = \frac{X_p}{Y_p}$ in (18) is determined by points $B_p = e^{j(\pi+\phi_m)}$ and $A_p = G(j\omega_p)$, the values of $\omega_g \in S_{\gamma\omega}$ are obtained from (17) solving the equation $\gamma = \gamma_g(\omega_g)$, parameters ω_n and δ are given by relations (19) and (20).

B) Design a lead-lag compensator $C(s)$ which satisfies constraints on the phase margin ϕ_m, the gain margin G_m and the phase crossover frequency ω_g. **Solution**: $\gamma = \frac{X_g}{Y_g}$ in (18) is determined by points $B_g = -1/G_m$ and $A_g = G(j\omega_g)$, the values of $\omega_p \in S_{\gamma\omega}$ are obtained from (17) solving equation $\gamma = \gamma_p(\omega_p)$, parameters ω_n and δ are given by relations (19) and (20).

C) Design a lead-lag compensator $C(s)$ which satisfies constraints on the phase margin ϕ_m, the gain margin G_m and the maximum allowable gain γ. **Solution**: γ is the minimum of the two values $\bar{\gamma}_p$ and $\bar{\gamma}_g$ that can be graphically determined on the Nyquist plane by drawing the circles $\mathscr{C}^-_{B_p\gamma_p}(j\omega)$ and $\mathscr{C}^-_{B_g\gamma_g}(j\omega)$ tangent to function $G(j\omega)$, see Fig. 6. The same values $\bar{\gamma}_p$ and $\bar{\gamma}_g$ can also be determined by finding the maximum points of the functions $\gamma_p(\omega_p)$ and $\gamma_g(\omega_g)$ defined in (18) and shown in Fig. 5. The frequencies ω_p and ω_g corresponding to value $\gamma = \min(\bar{\gamma}_p, \bar{\gamma}_g)$ can be substituted in (19) and (20) providing the parameters ω_n and δ of the lead-lag compensator $C(s)$.

D) Design a lead-lag compensator $C(s)$ which satisfies the gain margin G_m, the phase crossover frequency ω_g and the maximum allowable phase margin ϕ_m. **Solution**: $\gamma = \frac{X_g}{Y_g}$ in (18) is determined by points $B_g = -1/G_m$ and $A_g = G(j\omega_g)$. The value of γ completely defines the shape of circle $\mathscr{C}_{B\frac{1}{\bar{\gamma}}}(j\omega)$. The maximum value $\bar{\phi}_m$ of the phase margin ϕ_m can be graphically determined moving point $B_p = e^{j(\pi+\phi_m)}$ on the unit circle until $\mathscr{C}_{B\frac{1}{\bar{\gamma}}}(j\omega)$ is tangent to function $G(j\omega)$. The frequency ω_p of the tangent point substituted in (19) and (20) provides the parameters ω_n and δ of the compensator $C(s)$.

V. Numerical Examples

The graphical representations shown in Fig. 5 and Fig. 6 have been obtained referring to the following transfer function:

$$G(s) = \frac{1200(s+2)}{(s+1.5)^2(s+7)^2} \tag{26}$$

and solving the Design Problem (ϕ_m, G_m) subject to the following specifications: $\phi_m = 45°$, $G_m = 3$ and $\gamma = 0.282$.

The solutions of the Design Problem have been obtained as follows. The design specifications define points $B_p = e^{j225°}$ and $B_g = 0.333\,e^{j180°}$. The four solutions $(\omega_{pi}, \omega_{gj})$ of (17) can be graphically determined as shown in Fig. 5: $\omega_{pi} = \{4.82, 6.72\}$, $\omega_{gj} = \{8.45, 12.8\}$. The corresponding points on function $G(j\omega)$ are $A_{p1} = 3.4\,e^{-j147.1°}$, $A_{p2} = 1.89\,e^{-j169°}$, $A_{g1} = 1.17\,e^{j176.1°}$ and $A_{g2} = 0.44\,e^{j151.8°}$. By substitution in (19) and (20), we obtain only two acceptable and stable regulators $C_\gamma(s, \omega_p, \omega_g)$. The first one is obtained for $(\omega_{p1}, \omega_{g2})$, $\delta = 1.21$ and $\omega_n = 4.345$:

$$C_\gamma(s, \omega_{p1}, \omega_{g2}) = \frac{s^2 + 2.97s + 18.88}{s^2 + 10.5s + 18.88}. \tag{27}$$

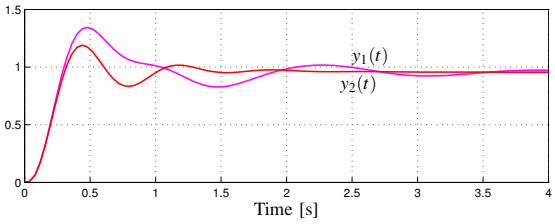

Fig. 7. Step responses $y_1(t)$ (magenta line) and $y_2(t)$ (red line) of the closed loop system when, respectively, regulators $C_\gamma(s,\omega_{p1},\omega_{g2})$ in (27) and $C_\gamma(s,\omega_{p2},\omega_{g2})$ in are used.

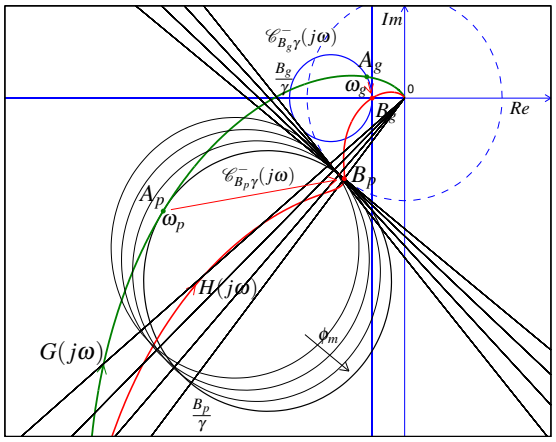

Fig. 8. Graphical solution of Design Problem *D*.

The second one is obtained for $(\omega_{p2},\omega_{g2})$, $\delta = 2.90$ and $\omega_n = 1.99$:

$$C_\gamma(s,\omega_{p1},\omega_{g2}) = \frac{s^2+3.27s+3.98}{s^2+11.58s+3.98}. \qquad (28)$$

The other solutions are not acceptable. The Nyquist plots of the loop gain transfer functions $H_{ij}(j\omega) = C_\gamma(j\omega,\omega_{pi},\omega_{gj})G(j\omega)$ are shown in Fig. 6. The step responses of the acceptable solutions are shown in Fig. 7.

Solution of the Design Problem C: the maximum $\gamma = \bar{\gamma}_p$ which satisfies the Design Problem *C* when $\phi_m = 45^\circ$ and $G_m = 3$ can be graphically determined drawing the circle $\mathscr{C}^-_{B_p\gamma_p}(j\omega)$ tangent in A_p to function $G(j\omega)$ as shown in Fig. 6. The obtained value is $\bar{\gamma}_p = 0.324$.

Solution of the Design Problem D: given the phase crossover frequency $\omega_{g2} = 12.8$ and the gain margin $G_m = 3$, the maximum phase margin $\bar{\phi}_m$ which satisfies the Design Problem *D* can be graphically determined as shown in Fig. 8. The obtained value is $\bar{\phi}_m = 51.75^\circ$. When phase margin ϕ_m increases from 40° to $\bar{\phi}_m$, function $\gamma_p(\omega)$ modifies its shape as shown in Fig. 9.

VI. Conclusion

A general form of lead-lag compensators which include real or complex zeros and poles has been considered. Necessary and sufficient conditions to

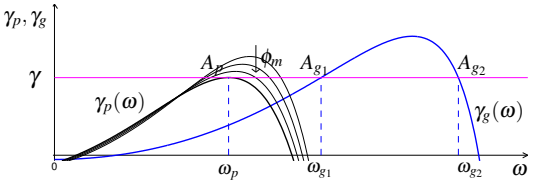

Fig. 9. Design problem *D*: function $\gamma_g(\omega)$ (blue line) and functions $\gamma_p(\omega)$ (black lines) for $\phi_m = \{40, 44, 48, 51.75\}$.

exactly satisfy gain and phase margins specifications have been proposed together with a simple graphical solution on the Nyquist plane. One of the main advantages of the proposed graphical solution over other graphical approaches, such as [13], is that it can be directly determined in the complex plane by the intersections of the frequency response of the plant and circles that can be easily done by ruler and compass. Moreover graphical approaches such as the one given in [13] can only deliver a subset of all the admissible solutions and some of them can lead to negative (and therefore infeasible) values of the compensator parameters. The presented results seem to be useful both for educational and industrial purposes.

References

[1] Weng Khuen Ho, Chang Chieh Hang and Lisheng S. Cao, *Tuning of PID controllers based on gain and phase margin specifications*. Automatica: 31(3):497-502, 1995.

[2] K.S. Yeung, K.W. Wong and K.L. Chen, *A Non Traial-and-Error Method for Lag-Lead Compensator Design*. IEEE Transactions on Education, E-41, no. 1, Feb. 1998.

[3] K.J. Aström and T. Hagglund, *Automatic Tuning of Simple Regulators with Specifications on Phase and Amplitude Margins*. Automatica: Vol. 20,No.5, 645-651, Sep. 1984.

[4] Q.G. Wang, H.W. Fung ,Y. Zhang , *PID tuning with exact gain and phase margins*. ISA Trans., 38,243-249, 1999.

[5] Lee Ching-Hung, *A survey of PID controller design based on gain and phase margins*. International Journal of Computational Cognition: 2(3):63-100, 2004.

[6] W.C. Messner, M.D. Bedillion, L. Xia, D.C. Karns. *Lead and Lag Compensators with Complex Poles and Zeros: design formulas for modeling and loop shaping*. Control Systems Magazine, vol.27, no.1, pp.44-54, Feb 2007.

[7] S.S. Flores, A.M. Valle and B.A. Castillejo *Geometric Design of Lead/Lag Compensators Meeting a Hinf Specification*. ICEEE , Mexico City, Mexico, Sept 5-7, 2007.

[8] W. Messner, *Formulas for Asymmetric Lead and Lag Compensators*. American Control Conference, St. Louis, MO, USA, June 10-12, 2009.

[9] L. Ntogramatzidis, and A. Ferrante, *Exact Tuning of PID Controllers in Control Feedback Design*, IET Control Theory & Applications, In Press (accepted on 18-11-10).

[10] Charles L. Phillips. *Analytical Bode Design of Controllers.* IEEE Trans. on Education, E-28, no. 1, pp. 43–44, 1985.

[11] G. Marro and R. Zanasi, *New Formulae and Graphics for Compensator Design* , IEEE International Conference On Control Applications, Trieste, Italy, September 1-4, 1998.

[12] R. Zanasi, R.Morselli, *Discrete Inversion Formulas for the Design of Lead and Lag Discrete Compensators*, ECC, 23-26 August 2009, Budapest, Hungary.

[13] K.S. Yeung and K.H. Lee, *A universal design chart for linear time-invariant continuous-time and discrete-time compensators*, Education, IEEE Transactions on , vol.43, no.3, pp.309-315, Aug 2000.